PLASTER CHARACTERIZATION AT THE PPNB SITE OF YIFTAHEL (ISRAEL) INCLUDING THE USE OF [14]C: IMPLICATIONS FOR PLASTER PRODUCTION, PRESERVATION, AND DATING

Kristin M Poduska[1,2] • Lior Regev[2] • Francesco Berna[3] • Eugenia Mintz[4] • Ianir Milevski[5] • Hamudi Khalaily[5] • Steve Weiner[2] • Elisabetta Boaretto[4]

ABSTRACT. The Pre-Pottery Neolithic B (PPNB) site of Yiftahel, Israel, contains abundant plaster floors. We surveyed the states of preservation of the plasters using an infrared spectroscopic assay that characterizes the extent of disorder of the atoms in the calcite crystal lattice. We identified the 3 best-preserved plaster samples that had disorder signatures most similar to modern plaster. We then studied the surface layers, fine-grained matrices, and large aggregates of these samples using micromorphology, Fourier transform infrared (FTIR) microscopy, stable carbon and radiocarbon concentrations. Even though some of the plaster components have a geogenic appearance in micromorphology slides and in FTIR spectra, the ^{14}C analyses show that all components were exposed to high temperatures and as a result were equilibrated with the ^{14}C content of the atmosphere ~10,000 yr ago. This implies that the plasters at Yiftahel were produced entirely from heat-altered calcite. We also show that these plasters have undergone significant diagenesis. The plaster component with the most disordered atomic signature, and hence the most similar in this respect to modern plaster, did indeed produce a ^{14}C date close to the expected age.

INTRODUCTION

The Pre-Pottery Neolithic B (PPNB) is a period that is renowned for plaster production. This is exemplified by the site of Yiftahel (Lower Galilee, Israel), where large tracts of plaster floors were preserved in several different stratigraphic levels (Garfinkel 1987; Ronen et al. 1991; Marder et al. 2008; Milevski et al. 2008). Nearly 2000 m[2] have been excavated by archaeological and salvage expeditions over the last 25 yr, and these investigations have shown that the PPNB stratigraphy can be quite different from area to area. Nevertheless, the PPNB buildings display a rectilinear plan with mud-brick and/or stone walls. Elements present within the structures include constructed hearths, pits, installations, and burials. All structures have thick lime-plastered floors. The building entrances were narrow openings that also possessed plastered floors.

The arrangement of the buildings differs in each area of the site. It appears that the major area (Area I) underwent more dynamic change over time, possibly as a result of a series of destructions that occurred during the PPNB. In several places, building debris seems to have been exposed to extremely high temperatures. All of the buildings exhibited postholes, while numerous lumps of mud with branch and plants impressions were found strewn throughout the area. It may thus be conjectured that wooden pillars were utilized to support a roof comprised of branches. The site is dated by radiocarbon to the middle-late PPNB (8000–7000 cal BC) (Milevski et al. 2008), and this is consistent with the typologies of the lithic artifacts (Khalaily 2006; Barzilai 2010).

The plan and the structures at the site; the human, botanic, and animal remains; and the variety of craft activities, both for internal use and external interchange, all suggest that Yiftahel was a major site at the time. Yiftahel must be considered as a centrally located and integral component of a PPNB network of interacting sites.

[1]Department of Physics and Physical Oceanography, Memorial University of Newfoundland, St. John's A1B 3X7, Canada. Corresponding author. Email: kris@mun.ca.
[2]Department of Structural Biology, Weizmann Institute of Science, Rehovot 76100, Israel.
[3]Department of Archaeology, Boston University, 675 Commonwealth Ave, Boston, Massachusetts 02215, USA.
[4]Radiocarbon Dating and Cosmogenic Isotopes Laboratory, Kimmel Center for Archaeological Science, Weizmann Institute of Science, Rehovot 76100, Israel.
[5]Israel Antiquities Authority, PO Box 586, Jerusalem 91104, Israel.

Little is known about how plasters were prepared in the PPNB (Kingery et al. 1988; Goren and Goldberg 1991; Malinowski and Garfinkel 1991), in part because there is no definitive evidence of kilns or of the large volume of calcitic residue that would be expected to accompany plaster production on such a large scale (Ronen et al. 1991). Goren and Goring-Morris (2008) showed through an experimental archaeology study that lime kilns, and the associated calcitic material, degrade due to exposure to the elements and bioturbation, such that after 9 yr they are almost unrecognizable. An alternative explanation for the lack of evidence for PPNB lime kilns is that the large-scale plaster production could have occurred outside of the habitation areas that have been targeted in archaeological excavations. For these reasons, any insights that can be gained about plaster production processes from analyses of the plasters themselves are of much interest.

In modern contexts, lime plasters are produced by heating limestone above 750 °C to convert the $CaCO_3$ into calcium oxide (CaO) and carbon dioxide (Boynton 1980). When water is added to this heated product, the resulting slaked lime ($Ca(OH)_2$) can be combined with other constituents such as geogenic calcite or old plaster pieces to improve strength (Borrelli 1999). This multicomponent slurry slowly dehydrates and absorbs CO_2 from the atmosphere to reform as calcite. Complete dehydration can take years to occur, depending on the thickness of the plaster (Lindroos et al. 2007).

Plaster can, in principle, be dated by ^{14}C because the source of the carbon is from the atmospheric carbon dioxide that is taken up during the drying process that converts calcium hydroxide into calcite. Numerous investigations have shown, however, that there are difficulties in obtaining accurate dates from plasters (Van Strydonck et al. 1992; Sonninen and Jungner 2001; Lindroos et al. 2007; Heinemeier et al. 2010). These difficulties are not related to the ^{14}C measurement methods, but rather stem from the inherent complexity of the component mixtures involved in producing a calcite plaster. Aggregates added to the slaked lime to improve its mechanical properties and increase bulk are often geogenic limestone. This means that such aggregates contribute carbon to the specimen, but no [14]C. Because the plaster crystals themselves are more disordered at the atomic level (Poduska et al. 2011), they are relatively soluble and unstable. They therefore have the propensity to dissolve and recrystallize as more ordered calcite. If during this process exchange takes place with the atmosphere, then an inaccurate ^{14}C date is obtained. Attempts to circumvent this problem involve dating only the first fractions that dissolve in acid, on the assumption that they are derived mostly from the less stable original crystals (Sonninen and Jungner 2001; Lindroos et al. 2007).

In this study, we first assessed the atomic disorder of plaster samples from Yiftahel using infrared spectroscopy (Regev et al. 2010; Poduska et al. 2011). From these, we selected the 3 best-preserved samples, namely those with disorder signatures most similar to modern plaster. We then characterized these plaster samples using optical microscopy, electron microscopy, and infrared microscopy, and finally analyzed both the ^{14}C contents and the stable carbon isotopic compositions of different components of these plasters. In this way, we gained new information on the mode of plaster production, and new insights into the problems involved in dating such plasters.

MATERIALS AND METHODS

Archaeological Context

Yiftahel, located 8 km NW of Nazareth in the Lower Galilee region of Israel, is situated near large amounts of limestone and chalk, which makes it a convenient location for plaster production (Figure 1). Dolomite, which is known to make inferior plasters, would not have been immediately available, since the closest sources are at least 10 km away.
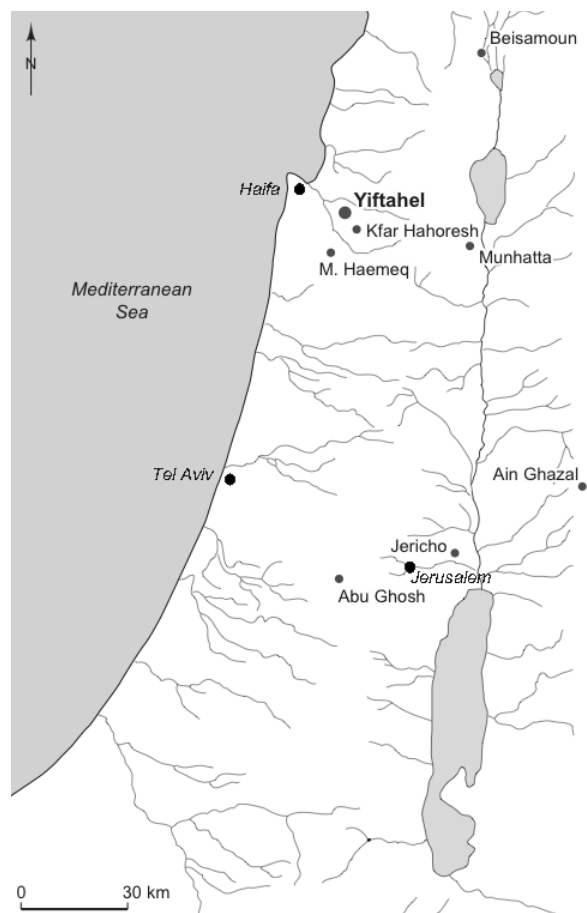
Figure 1 Map of PPNB sites with the location of Yiftahel shown in bold type. The names in italics provide references for landmarks in modern Israel.

Microstratigraphy

Plaster specimens were embedded in epoxy, cut with a rock saw, and polished to optical smoothness before being bonded to a glass slide (76 × 50 mm) with Epofix™ resin. Thin sections (30–60 μm thickness) were then produced by incremental polishing (Buehler PetroThin® Sectioning System). These slides were subsequently examined with a polarized light microscope (Nikon Eclipse E600POL).

Fourier Transform Infrared Spectroscopy (FTIR)

Measurements were made on thin (<1 mm) pellets produced from ~0.1 mg of plaster and ~40 mg KBr that was mixed in an agate mortar, hand-powdered, and then pressed using a manual hydraulic press (Specac). Infrared spectra were collected with a Thermo-Nicolet 380 spectrometer (4 cm^{-1} resolution, 32 scans). Baselines and subsequent peak-height analyses of the ν_3 (1420 cm^{-1}), ν_2 (874 cm^{-1}), and ν_4 (713 cm^{-1}) peaks followed procedures in earlier publications (Chu et al. 2008). The grinding curve analysis method (Regev et al. 2010; Poduska et al. 2011) provided information about the degree of crystallinity in different parts of each plaster sample.

FTIR Microscopy

Reference samples (sparitic and micritic limestone, fresh and heated chalk, and experimentally produced plaster) and archaeological plaster processed in thin section were analyzed by FTIR microspectroscopy using a Nicolet Spectra Tech Continuμm™ IR microscope attached to a Nicolet Nexus 460 spectrometer. Spectra of particles with diameters near 150 μm were collected in transmission and total reflectance mode between 4000 and 450 cm^{-1} at 8 cm^{-1} resolution using a Reflectocromat 15× objective. Prior to IR measurements, the thin-section surfaces were lapped with 1-μm grit diamond lapping film using a Buehler EcoMet/AutoMet® 250 polisher/grinder.

Stable Carbon Isotope Analysis and Radiocarbon Dating

All samples were prepared at the Radiocarbon and Cosmogenic Isotopes Laboratory in the Kimmel Center of Archaeological Science at the Weizmann Institute of Science (Rehovot, Israel). Twenty to 30 mg of different portions of each sample were crushed and dissolved in phosphoric acid for CO_2 extraction. A portion of the CO_2 was used for $\delta^{13}C$ measurements, and the rest was converted into graphite for accelerator mass spectrometry (AMS) according to the method described by Yizhaq et al. (2005). The carbon content of the samples ranged from 11.6–12.3%, which is very close to the value expected for pure calcite (12.0%). ^{14}C ages are reported in conventional ^{14}C years in accordance with international convention (Stuiver and Polach 1977). All calculated ^{14}C ages have been corrected for fractionation to make the results equivalent with the standard $\delta^{13}C$ value of –25‰ (wood). Calibrated ages in calendar years have been obtained from the data of Reimer et al. (2009) through OxCal v 4.1.5 software (Bronk Ramsey 1995, 2001).

RESULTS

Forty plaster samples were collected from floors of Pre-Pottery Neolithic B strata in Area I at Yiftahel (Milevski et al. 2008). Twenty-five of the 40 samples have good stratigraphic information and were considered for subsequent study. From these, we chose 3 samples for detailed analysis based on infrared spectroscopic analysis that showed that they have relatively disordered calcite crystals that are consistent with well-preserved plaster. Sample L5118, from Building 501, was extracted between 2 pits with ash and under a thick burnt brick. YIF142 was also from Building 501. L5512 was from Building 550, and it was located under brick material that had been exposed to elevated temperatures.

Plaster Structure, Composition, and Layer Differences

Polished cross-sections (Figure 2) show that Yifthael plasters have thin characteristic white, fine-grained top layers (2–5 mm thick) that include microscopic aggregates. Below the white surface layer are yellow-red layers that contain differently sized and shaped aggregates ranging from microscopic to large (mm–cm sized) inclusions embedded in a fine-grained matrix. FTIR data indicate that all aliquots from both top and bottom layers are comprised almost entirely of calcite. This was confirmed by scanning electron microscopy and energy-dispersive X-ray analyses. The thin surface layer shows the presence of reddish-brown fine material in some areas that shows typical kaolinite and smectite IR absorptions (Figure 4b).

Optically thin sections, viewed with polarized light microscopy, provide additional information based on the birefringent characteristics of calcite. Figure 3 shows representative images of thin sections viewed through crossed polarizers. Figure 3a shows a micritic top layer that is indicative of a lime plaster, as well as sparitic infillings in cracks that suggest secondary calcite was deposited by diagenetic processes. These sparry calcite infillings are also evident in the bottom layers of the plas-
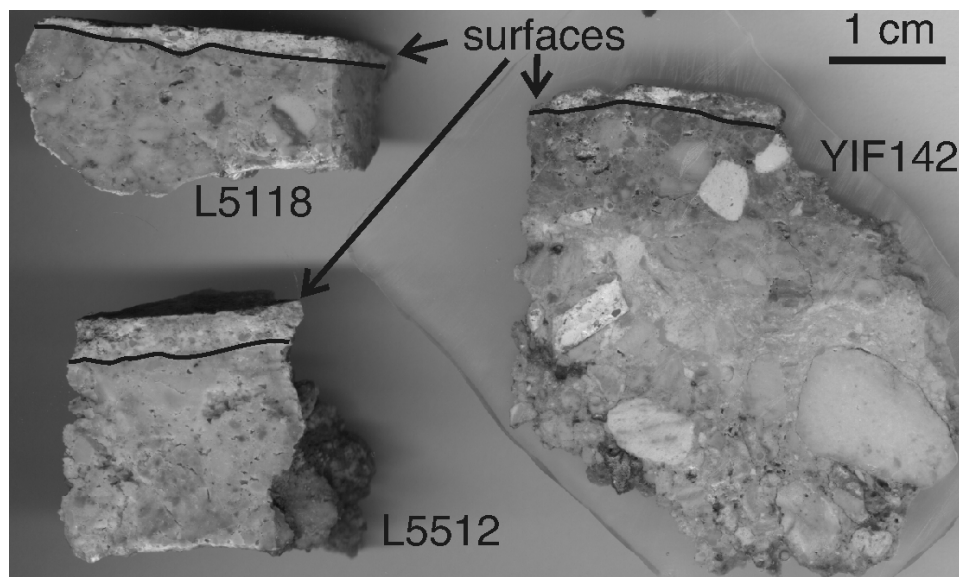
Figure 2 Polished cross-sections of 3 representative plaster floors. The fine-grained white surface layers are denoted with arrows.

ters (Figure 3b), which are comprised of discrete aggregates and binder material. Some of these aggregates appear to be fragments of chalk and micrite, and some show fossilized foraminifera, which attests to their geogenic origins.
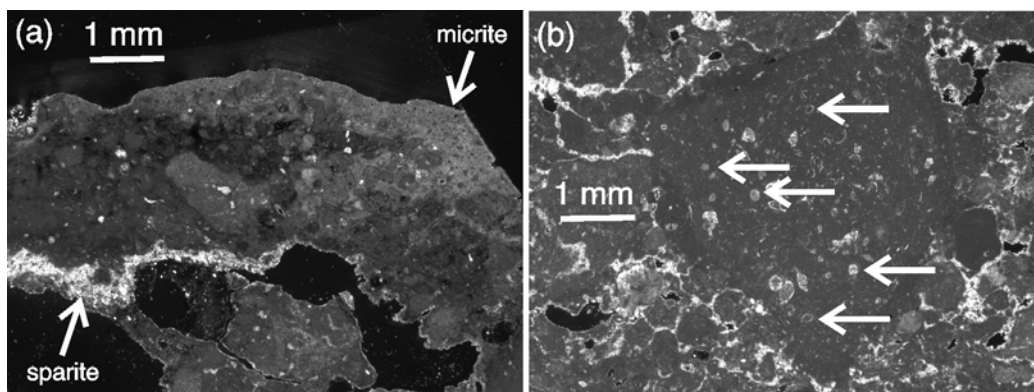

Figure 3 (a) Thin sections show a micritic thin surface layer and sparitic infillings in cracks. (b) Some fragments in the bottom layer show evidence of fossilized foraminifera, indicated by arrows, which is indicative of fossiliferous micrite.

Micro-FTIR measurements of standard calcitic material processed in thin sections show some appreciable differences in the ν_3 carbonate IR reflectance band (1550 to 1405 cm^{-1}) between sparitic and micritic limestone and between fresh and heated chalk (Figure 4a). Interestingly, these reflectance patterns are also recognizable among the thin micritic top layer of plaster and the sparitic infillings (Figure 4b). Specifically, the IR reflectance patterns of the micritic surface layer compare well with spectra from experimental plaster (Figure 4a), while the IR patterns of the aggregates analyzed are comparable to fresh chalk and micritic limestone, indicating that if these aggregates were heated they probably did not reach high enough temperatures (~800 °C) to completely transform

into pyrogenic calcite. This hypothesis is supported by the presence of the fossil foraminifera that would have been recrystallized after complete calcination (Goren and Goldberg 1991).
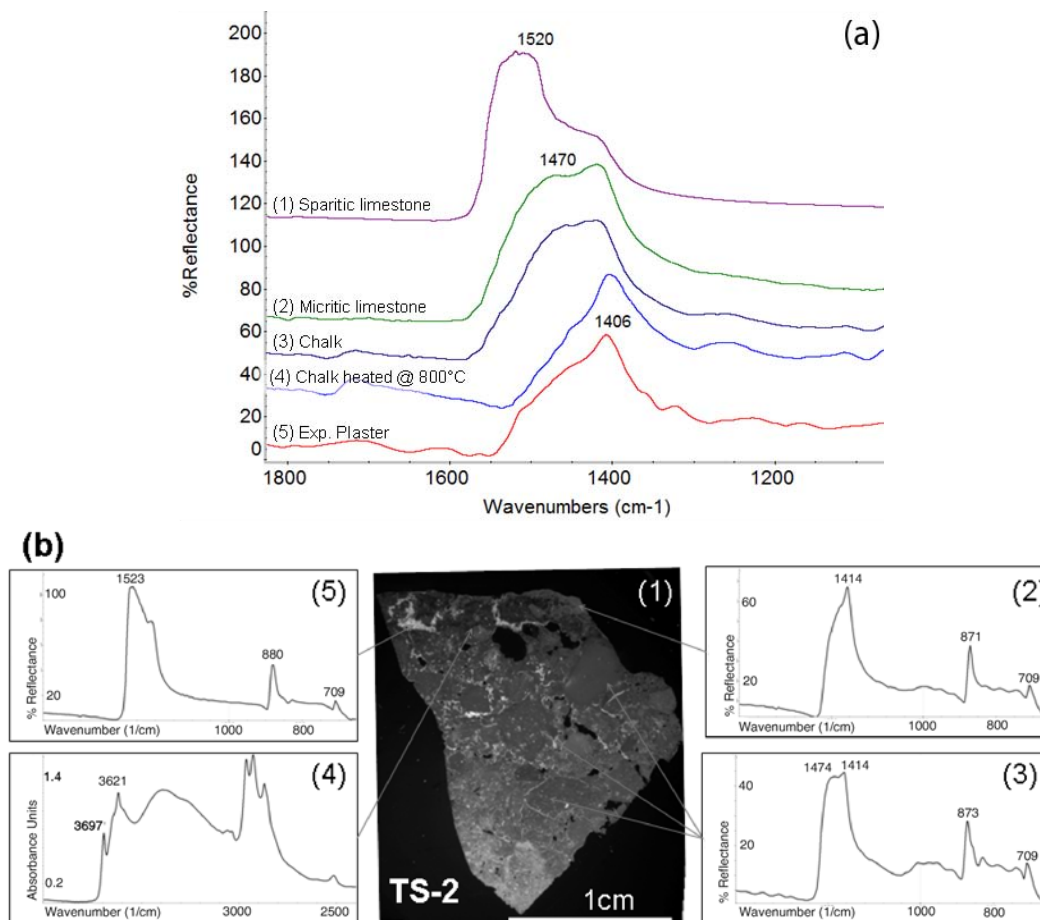

Figure 4 (a) FTIR reflectance spectra of the $v_3 CO_3$ bands collected from several reference calcite materials processed in thin section: (1) sparitic limestone (Ward's) showing stronger intensity at 1520 cm^{-1}; (2) micritic limestone (Ward's) showing a broad absorption at 1470 cm^{-1} and a sharper absorption at 1405 cm^{-1}; (3) chalk (Ward's) showing similar FTIR reflectance patterns to micrite; (4) chalk (Ward's) heated for 2 hr at 800 °C. Notice the disappearance of the broad band at 1470 cm^{-1}; (5) experimental plaster. (b) Cross-polarized light scan of archaeological plaster sample YIF142b processed in thin section (1) and representative FTIR spectra of different particles: (2) FTIR reflectance spectrum of micritic plaster layer showing high similarity with spectra of experimental plaster and calcined chalk (Figure 4a: 4, 5); (3) FTIR reflectance spectrum of fragments of micritic limestone and chalk showing similarity with fresh micritic limestone and chalk (Figure 4a: 2, 3); (4) FTIR transmission spectrum of reddish brown clay particles showing kaolinite and illite-smectite absorption at 3620 and 3695 cm^{-1}; (5) FTIR reflectance spectrum of sparitic calcite infilling that is similar to reference sparite.

We analyzed all 25 samples with good stratigraphic information using FTIR spectroscopy to compare the atomic order/disorder properties of the calcite crystals from the top layers, the binder, and aggregate material in the lower layers using the grinding curve analysis approach described by Regev et al. (2010). The 3 best samples, which are shown in Figure 2, each have a thin top layer that contains calcite that is less crystalline than the calcite contained in the bottom layers. These grinding curve comparisons are shown in Figure 5 for top (a) and bottom (b) layers. The crystallinity differ-

ences we observe could mean that the bottom layers have undergone more diagenetic recrystalliza-tion, or that the bottom layers contain highly crystalline geogenic inclusions. Surprisingly, there appears to be similar extents of disorder in the aggregates and binders in all 3 samples (Figure 5b). The top layers contain slightly more crystalline material than fresh plaster (Figure 5a). Of the 3 sam-ples shown in Figure 5, the top layer of sample L5118 has a grinding curve closest to modern plaster and therefore should be the best-preserved sample.
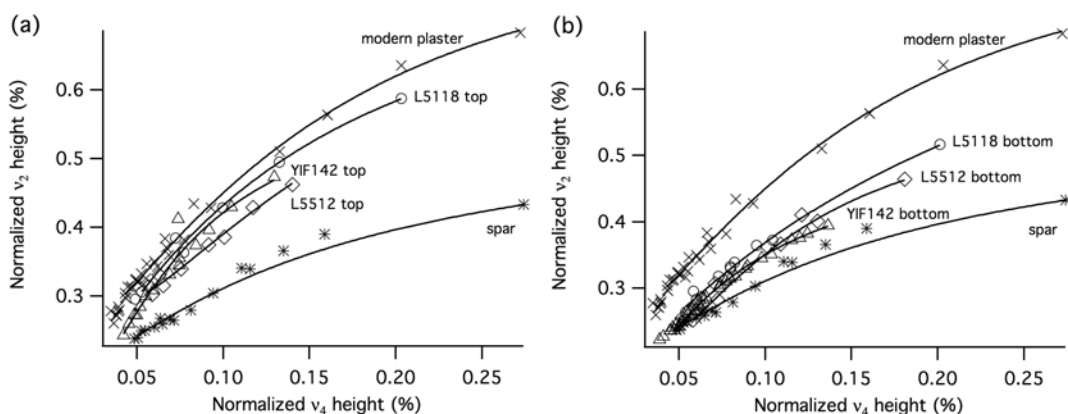

Figure 5 Analysis of FTIR spectral peak ratios enable assessments of atomic order/disorder differences as compared to modern plaster (least crystalline) and geogenic spar calcite (most crystalline): (a) shows that the top layers are less ordered (more like modern plaster), while (b) shows that the bottom layers are more ordered (more similar to spar calcite).

Stable Carbon Isotope and Radiocarbon Results

Table 1 summarizes the isotopic data obtained from the 3 Yiftahel plaster specimens. All of the ^{14}C data cluster between 8000 and 12,000 yr BP uncal (9000–14,000 cal BP), which includes the expected age of the site, 9000–10,000 yr cal BP (Milevski et al. 2008). We do, however, note that the top layer of the plaster L5518, which had a grinding curve closest to the modern plaster, produced a date within the expected range and has the lightest δ^{13}C of –19.3‰. Based on the consistent and considerable amount of modern carbon present in all specimens, there is no evidence that the aggre-gates within the plaster are unaltered geogenic limestone.

Table 1 Summary of isotopic data for Yiftahel plaster specimens. The ages are quoted with an uncertainty of ±1 σ.

Lab nr	Sample description	% C	pMC	^{14}C age BP uncal (yr)	δ^{13}C (‰)
RTS 6229	L5512 binder	11.9 ± 0.2	35.1 ± 0.3	8405 ± 70	–10.3 ± 0.4
RTS 6230	L5512 aggregate	12.3 ± 0.2	26.5 ± 0.3	10,670 ± 80	–9.8 ± 0.1
RTS 6231	L5518 top	11.7 ± 0.2	32.3 ± 0.3	9080 ± 75	–19.3 ± 0.2
RTS 6232	L5518 binder	12.2 ± 0.2	28.1 ± 0.3	11,870 ± 95	–9.1 ± 0.4
RTS 6233	L5518 aggregate	12.2 ± 0.2	24.3 ± 0.3	11,380 ± 85	–9.2 ± 0.5
RTT 6082	YIF142 top	10.7 ± 0.2	27.2 ± 0.3	10,380 ± 250	–11.3 ± 0.1
RTT 6083	YIF142 binder	11.4 ± 0.2	31.2 ± 0.3	8580 ± 240	–7.6 ± 0.1
RTS 6234-1	YIF142 aggregate 1	12.0 ± 0.2	33.0 ± 0.3	8960 ± 75	–8.6 ± 0.5
RTS 6234-2	YIF142 aggregate 2	11.6 ± 0.2	38.0 ± 0.3	7730 ± 70	–8.3 ± 0.5

DISCUSSION

The ^{14}C results clearly show that all of the calcite in these plasters equilibrated with the atmosphere sometime around 10,000 yr ago. This is surprising given the fact that the microstructural appearance and infrared spectral properties appear to suggest that these plasters include some geogenic components. Nevertheless, there are plausible explanations that account for all of these ^{14}C, microstructural, and infrared spectral data.

Plaster Production Processes at Yiftahel

One scenario that could account for the above observations is that all of the materials used for the production of these plasters were heated above 750 °C. After heating for a sufficient time at this temperature, limestone calcite would degrade into CaO. After cooling and hydration, it would then transform into calcium hydroxide (slaked lime). It is possible that partially degraded limestone could have been used as aggregates for the bottom layer of the plaster, together with fine-grained slaked lime. If the limestone was heated long enough to change ^{14}C levels but not long enough to change the crystallinity of the material, then this scenario accounts for both the infrared spectroscopic data and the ^{14}C data that indicate partial or total re-equilibration with the atmosphere shortly after production.

It is possible that the plaster, as produced, could have contained a mixture of both fully reacted and partially reacted lime. In this scenario, it is possible that part of the lime equilibrated with atmospheric CO_2 at a much later time. A mixture of old and new lime could, in principle, produce ^{14}C levels that are consistent with those we observe, assuming that the calcite formed from the newer lime counteracts the dead carbon of the truly geogenic calcite. However, it would be quite fortuitous for this mixture to give uniform carbon levels throughout different regions of several different plaster floors at this site. Furthermore, the crystallinity differences between the new and geogenic plaster would also lead to distinct differences in the infrared spectra that we do not see. Thus, it seems less likely that this scenario is relevant for the Yiftahel plasters we have analyzed.

Variation in Radiocarbon Values: Preservation vs. Differential Heating-Related Degradation

Partial degradation of calcite to lime at high temperatures will result in a mixture of calcite, some of which is equilibrated with the CO_2 in the atmosphere (via the associated water) and some geogenic calcite with no [14]C. The geogenic portions of the samples will have more ordered calcite crystals than the heated, atmospherically equilibrated portions.

Diagenetic processes that involve dissolution and reprecipitation can change both the degree of crystallographic order within calcite crystallites and the percentage of modern carbon. The more soluble, disordered crystals that had been heated are more prone to dissolve and reprecipitate. The resulting crystals have a higher degree of order, and they will also have younger apparent ages if ^{14}C levels re-equilibrate with the atmosphere at the time of reprecipitation. In our plaster samples, the sparite crystals in the veins shown in Figure 3 are an example of a product of this kind of diagenetic dissolution and reprecipitation. The fact that the uncalibrated ^{14}C ages are in a relatively restricted range and are older than or similar to the expected ones indicates that the diagenesis happened close to the time of the plaster formation rather than being a continuous process through time. This also implies that in Yiftahel samples the plaster is a stable material once it is formed and does not change significantly over time.

We conclude that the effects of differing extents of carbonation and diagenesis make it impossible to predict *a priori* which samples are best for dating. However, we do note that the sample with the

most disordered crystals, which also had the lightest stable isotope values, gave a date closest to the range expected. Nevertheless, we cannot be sure that this criterion of high disorder in the calcite crystals is sufficient to guarantee accurate dates for samples for which the age is unknown.

CONCLUSIONS

Plaster samples from Yiftahel were produced entirely from lime plaster, and other components that retain a geogenic appearance, even though they were exposed to high temperatures and were thus equilibrated with the ^{14}C content of the atmosphere around 10,000 yr ago. The calcite crystals of the plaster have undergone considerable diagenesis. The one sample with an atomic disorder signature most similar to modern plaster produced a ^{14}C date closest to the expected age. Our findings point to the value of exploring applications of ^{14}C in archaeology beyond dating and chronology.

ACKNOWLEDGMENTS

REFERENCES

Barzilai O. 2010. *Social Complexity in the Southern Levantine PPNB as Reflected Through Lithic Studies. The Bidirectional Blade Industries*. BAR International Series 2180. Oxford: Archaeopress.

Borrelli E. 1999. Binders. In: *ARC Laboratory Handbook, ICCROM, Conservation of Architectural Heritage, Historic Structures and Materials*. Rome: IC-CROM. Available at http://www.iccrom.org/pdf/ICCROM_14_ARCLabHandbook02_en.pdf. p 1–9.

Boynton RS. 1980. *Chemistry and Technology of Lime and Limestone*. New York: John Wiley & Sons.

Bronk Ramsey C. 1995. Radiocarbon calibration and analysis of stratigraphy: the OxCal program. *Radiocarbon* 37(2):425–30.

Bronk Ramsey C. 2001. Development of the radiocarbon calibration program. *Radiocarbon* 43(2A):355–63.

Chu V, Regev L, Weiner S, Boaretto E. 2008. Differentiating between anthropogenic calcite in plaster, ash and natural calcite using infrared spectroscopy: implications in archaeology. *Journal of Archaeological Science* 35(4):905–11.

Garfinkel Y. 1987. Yiftahel: a Neolithic village from the Seventh Millennium B.C. in Lower Galilee, Israel. *Journal of Field Archaeology* 14(2):199–212.

Goren Y, Goldberg P. 1991. Petrographic thin sections and the development of Neolithic plaster production in Northern Israel. *Journal of Field Archaeology* 18(1):131–8.

Goren Y, Goring-Morris AN. 2008. Early pyrotechnology in the Near East: experimental lime-plaster production at the Pre-Pottery Neolithic B site of Kfar HaHoresh, Israel. *Geoarchaeology: An International Journal* 23(6):779–98.

Heinemeier J, Ringbom Å, Lindroos A, Sveinbjörnsdóttir ÁE. 2010. Successful AMS ^{14}C dating of non-hydraulic lime mortars from the Medieval churches of the Åland Islands, Finland. *Radiocarbon* 52(1):171–204.

Khalaily H. 2006. Lithic traditions during the Late Pre-Pottery Neolithic B and the question of the Pre-Pottery Neolithic C in the Southern Levant [unpublished PhD thesis]. Ben-Gurion University of the Negev, Beersheva. In Hebrew with English summary.

Kingery WD, Vandiver P, Pricket M. 1988. The beginning of pyrotechnology, part II: production and use of lime and gypsum plaster in the Pre-Pottery Neolithic Near East. *Journal of Field Archaeology* 15(2):219–44.

Lindroos A, Heinemeier J, Ringbom Å, Braskén M, Sveinbjörnsdóttir Á. 2007. Mortar dating using AMS ^{14}C and sequential dissolution: examples from Medieval, non-hydraulic lime mortars from the Åland Islands, SW Finland. *Radiocarbon* 49(1):47–67.

Malinowski R, Garfinkel Y. 1991. Prehistory of concrete. *Concrete International* 13(3):62–8.

Marder O, Khalaily H, Milevski I, Eisenberg E, Sklar-Parnes D, Le Dosseur G. 2008. Two hafted tools from PPNB sites of the Southern Levant. *Neo-Lithics* 2:26–7.

Milevski I, Khalaily H, Getzov N, Hershkovitz I. 2008. The plastered skulls and other PPNB finds from Yiftahel, Lower Galilee (Israel). *Paléorient* 34(2):37–46.

Poduska KM, Regev L, Boaretto E, Addadi L, Weiner S, Kronik L, Curtarolo S. 2011. Decoupling local disorder and optical effects in infrared spectra: differentiating between calcites with different origins. *Advanced Materials* 23(4):550–4.

Regev L, Poduska KM, Addadi L, Weiner S, Boaretto E. 2010. Distinguishing between calcites formed by different mechanisms using infrared spectrometry: ar-

chaeological applications. *Journal of Archaeological Science* 37(12):3022–9.

Reimer PJ, Baillie MGL, Bard E, Bayliss A, Beck JW, Blackwell PG, Bronk Ramsey C, Buck CE, Burr G, Edwards RL, Friedrich M, Guilderson TP, Hajdas I, Heaton TJ, Hogg AG, Hughen KA, Kaiser KF, Kromer B, McCormac FG, Manning S, Reimer RW, Richards DA, Southon JR, Talamo S, Turney CSM, van der Plicht J, Weyhenmeyer CE. 2009. IntCal09 and Marine09 radiocarbon age calibration curves, 0–50,000 years cal BP. *Radiocarbon* 51(4):1111–50.

Ronen A, Bentur A, Soroka I. 1991. A plastered floor from the Neolithic village, Yiftahel (Israel). *Paléorient* 17(2):149–55.

Sonninen E, Jungner H. 2001. An improvement in preparation of mortar for radiocarbon dating. *Radiocarbon* 41(2A):271–3.

Stuiver M, Polach HA. 1977. Discussion: reporting of ^{14}C data. *Radiocarbon* 19(3):355–63.

Van Strydonck MJY, van der Borg K, de Jong AFM, Keppens E. 1992. Radiocarbon dating of lime fractions and organic material from buildings. *Radiocarbon* 34(3):873–9.

Yizhaq M, Mintz G, Cohen I, Khalaily H, Weiner S, Boaretto E. 2005. Quality controlled radiocarbon dating of bones and charcoal from the early Pre-Pottery Neolithic B (PPNB) of Motza (Israel). *Radiocarbon* 47(2):193–206.